Published in final edited form as:
Skin Pharmacol Physiol. 2013 ; 26(1): 36–44. doi:10.1159/000343175.

Sphingoid bases are taken up by *Escherichia coli* and *Staphylococcus aureus* and induce ultrastructural damage

Carol L. Fischer[a], **Katherine S. Walters**[b], **David R. Drake**[a,c], **Derek R. Blanchette**[a], **Deborah V. Dawson**[a,d], **Kim A. Brogden**[a,e], and **Philip W. Wertz**[*,a,f]

[a]Dows Institute for Dental Research, Radiology & Medicine, College of Dentistry, The University of Iowa, Iowa City, IA 52242, USA

[b]Central Microscopy Research Facility, Radiology & Medicine, College of Dentistry, The University of Iowa, Iowa City, IA 52242, USA

[c]The Department of Endodontics, Radiology & Medicine, College of Dentistry, The University of Iowa, Iowa City, IA 52242, USA

[d]The Department of Pediatric Dentistry, Radiology & Medicine, College of Dentistry, The University of Iowa, Iowa City, IA 52242, USA

[e]Department of Periodontics, Radiology & Medicine, College of Dentistry, The University of Iowa, Iowa City, IA 52242, USA

[f]The Department of Oral Pathology, Radiology & Medicine, College of Dentistry, The University of Iowa, Iowa City, IA 52242, USA

Abstract

Sphingoid bases found in the outer layers of the skin exhibit antimicrobial activity against Gram-positive and Gram-negative bacteria. We investigated the uptake of several sphingoid bases by *Escherichia coli* and *Staphylococcus aureus*, and assessed subsequent ultrastructural damage. *E. coli* and *S. aureus* were incubated with D-sphingosine, dihydrosphingosine, or phytosphingosine at ten times their MIC for 0.5 h and 4 h, respectively, to kill 50% of viable bacteria. Treated bacterial cells were immediately prepared for SEM, TEM, and analyzed for lipid content by QTLC. *E. coli* and *S. aureus* treated with sphingoid bases were distorted and their surfaces were concave and rugate. Significant differences were observed in the visual surface area relative to controls for both *E. coli* and *S. aureus* when treated with dihydrosphingosine and sphingosine ($p<0.0001$) but not phytosphingosine. While sphingoid base-treated *S. aureus* exhibited disruption and loss of cell wall and membrane, *E. coli* cytoplasmic membranes appeared intact and the outer envelope uncompromised. Both *E. coli* and *S. aureus* cells contained unique internal inclusion bodies, likely associated with cell death. QTLC demonstrated extensive uptake of sphingoid bases by the bacteria. Hence, sphingoid bases induce both extracellular and intracellular damage and cause intracellular inclusions that may reflect lipid uptake.

Keywords

Antimicrobial lipids; sphingoid bases; sphingolipids; *Escherichia coli*; *Staphylococcus aureus*; ultrastructure; electron microscopy

[*]Corresponding author Philip W. Wertz, Ph.D., Professor, Department of Oral Pathology, Radiology & Medicine and Dows Institute for Dental Research, N449 DSB, College of Dentistry, 801 Newton Road, The University of Iowa, Iowa City, IA 52242, Tel: +1 (319) 335-7409; Fax: +1 (319) 335-8895, philip-wertz@uiowa.edu.

No conflict of interest exists.

Introduction

Sphingoid bases and neutral lipids are present in the stratum corneum where they likely contribute to the permeability and innate immunologic barriers of the skin [1,2]. Included among these lipids are fatty acids, derived from sebaceous triglycerides, and free sphingosine and dihydrosphingosine, derived from epithelial sphingolipids via hydrolytic enzymes. Although the antibacterial activity of these common lipids against both Gram-positive and Gram-negative bacteria has been established the mechanisms of action have not yet been firmly established.

D-sphingosine, phytosphingosine, and dihydrosphingosine are all similar in structure. Sphingosine (C18:1) is a long chain unsaturated fatty alcohol with a single trans double bond between C4 and C5, hydroxyl groups on C1 and C3, and an amino group on C2. Dihydrosphingosine (C18:0) is sphingosine's saturated analog. Both mediate a variety of cellular processes [3-7], through the inhibition of protein kinase C (PKC) [8]. Phytosphingosine (C18:0) is structurally similar to dihydrosphingosine with the exception of a hydroxyl group at C4. Phytosphingosine also mediates a variety of cellular processes and has anti-proliferative and anti-inflammatory properties [9,10].

D-sphingosine, dihydrosphingosine, and phytosphingosine exhibit varying degrees of antimicrobial activity [10-14] and are both lipid-specific and microorganism-specific against a variety of Gram-positive and Gram-negative bacteria [15-18]. Bibel and colleagues showed that these sphingoid bases are highly active against Gram-positive bacteria and fungi, but relatively inactive against Gram-negative bacteria. Based on studies including L-forms of *S. aureus*, the site of activity was suggested to be the cell wall. Electron microscopy showed cell wall lesions, disruption of the membrane, and leakage of cellular content [13].

Recently, we found that D-sphingosine, dihydrosphingosine, and phytosphingosine are active (MIC range 0.7 – 31.3 μg/ml) against *E. coli, S. aureus, Corynebacterium bovis, Corynebacterium striatum, Corynebacterium jeikium, Streptococcus sanguinis, Streptococcus mitis,* and *Fusobacterium nucleatum* but not against *Serratia marcescens* and *Pseudomonas aeruginosa* (MIC >500 μg/ml) [18]. Kinetics assays revealed that complete killing is achieved in as little as 0.5 h for some lipid-bacteria combinations but up to 24 h are required with other combinations. Although the antibacterial activity of these common sphingoid bases against both Gram-positive and Gram-negative bacteria has been established, the mechanisms of action have not yet been firmly established.

In this study, we begin to assess lipid activity against a representative Gram-positive and Gram-negative bacteria: *S. aureus,* an opportunistic skin pathogen contributing to a wide variety of diseases leading to an estimated 478,000 hospitalizations and 11,000 deaths in the United States annually[19], and *E. coli,* another contributor to skin and soft tissue infections [20,21]. Similar to the results of Bibel and colleagues, we show that sphingoid bases induce ultrastructural damage. Furthermore, we show that 1) sphingoid bases accumulate in the bacterial cell; 2) sphingoid bases induce differential ultrastructural changes in representative Gram-positive and Gram-negative bacteria; and 3) sphingoid bases induce the presence of intracellular inclusions. The combination of these ultrastructural changes indicates a need for further study into potential mechanisms for their antimicrobial activity against microorganisms.

Materials and Methods

Bacterial species and growth conditions

E. coli ATCC® 12795™ and *S. aureus* ATCC® 29213™ were grown for 3 h in Mueller Hinton broth (Difco Laboratories, Detroit, MI) at 37°C. Bacterial cell suspensions were adjusted to contain 1×10^8 CFU/ml (0.108 O.D., 600 nm, Spectronic 20D+, Thermo Fisher Scientific, Inc., Waltham, MA). For scanning electron microscopy, suspensions were then serially diluted to 1×10^5 CFU/ml before treatment and for transmission electron microscopy, suspensions were left at 1×10^8 CFU/ml.

Preparation of lipids

D-sphingosine, dihydrosphingosine, and phytosphingosine were obtained from Sigma Chemical Company (St Louis MO). Lipids were dissolved in a chloroform/methanol solution (2:1), and purity was confirmed by thin layer chromatography. Dried lipids were suspended in sterile 0.14 M NaCl to make a 1.0 mg/ml stock solution. The lipid samples were sonicated in 5 min increments to suspend the lipid, and diluted to the desired concentrations using 0.14 M NaCl.

Preparation of lipid-damaged bacterial cells

Broth cultures of *E. coli* and *S. aureus* were incubated with D-sphingosine, dihydrosphingosine, or phytosphingosine at 10X the previously determined MIC for 0.5 h (*E. coli* treatments) and 4 h (*S. aureus* treatments) at 37°C [18]. *E. coli* was treated with either 39 μg/ml phytosphingosine, 104 μg/ml sphingosine, or 312 μg/ml dihydrosphingosine. *S. aureus* was treated with either 13 μg/ml phytosphingosine, 16 μg/ml sphingosine, or 20 μg/ml dihydrosphingosine. In order to visualize cells in various stages of death, incubation times were based on killing kinetics [18] so that each suspension contained both viable (<50%) and non-viable (>50%) cells.

Scanning electron microscopy

After treatment with lipids, *E. coli* and *S. aureus* were layered on a membrane, fixed in 2.5% glutaraldehyde in 0.1 M sodium cacodylate buffer, pH 7.4, for 1 h in an ice bath and washed twice in 0.1 M sodium cacodylate buffer, pH 7.4, for 4 min. Samples were then further fixed in 1% osmium tetroxide for 30 min, washed twice in double distilled water, and dehydrated in a series of 25%, 50%, 75%, 95%, and absolute ethanol solutions followed by hexamethyldisilizane. Membranes containing *E. coli* or *S. aureus* were then mounted on stubs, sputter coated with gold and palladium, and examined with a Hitachi S-4800 scanning electron microscope (Hitachi High-Technologies Canada, Inc., Toronto, Ontario Canada).

Transmission electron microscopy

After treatment with lipids, *E. coli* and *S. aureus* were fixed in 2.5% glutaraldehyde in 0.1 M sodium cacodylate buffer, pH 7.4, for 1 h in an ice bath and washed twice in 0.1 M sodium cacodylate buffer, pH 7.4, for 20 min. After fixation, the organisms were pelleted by centrifugation and suspended in warm 0.9% agarose in 0.1 M sodium cacodylate buffer, pH 7.4. The agarose was diced into 1 mm cubes and washed twice in 0.1 M sodium cacodylate buffer, pH 7.4, for 20 min. Cubes of agarose containing treated *E. coli* or *S. aureus* were then treated with 1% osmium tetroxide for 1 h, washed twice in 0.1 M sodium cacodylate buffer, pH 7.4, for 20 min, dehydrated in a series of 30%, 50%, 70%, 95%, and absolute ethanol solutions, cleared in propylene oxide, infiltrated in a propylene oxide-Epon mixture (1:1), embedded in Epon, and polymerized at 60°C for 48 h. Ultrathin sections were cut, placed on formvar-coated nickel grids, and then stained with 5% uranyl acetate and

Reynold's lead citrate. Samples were examined in a JEOL JEM-1230 transmission electron microscope (JEOL USA, Inc., Peabody, MA USA).

Cell dimensions and statistical analysis

Cells were randomly selected and photographed. To quantitate the observed effects of lipid treatments on cells, we measured cell dimensions using ImageJ. For *E. coli,* length (L) and width (W) measurements were taken across the approximate center of each bacterium. For *S. aureus,* vertical diameter measurements (d) were taken across the approximate center of each cell. Analyses are based on a minimum of 10 measurements for each treatment/ organism combination.

Visible surface areas of *E. coli* (L × W) and *S. aureus* (πr^2, where r = d/2) were computed as a method of examining treatment-induced change in overall bacterial size. The nonparametric Kruskal-Wallis test was employed with a 5% level of significance to test the null hypothesis that the distribution of visual surface areas is the same for all the treatment groups designated. Pairwise comparisons among the four treatment groups within each bacterial species were performed using the exact Wilcoxon Rank Sum test. The Bonferroni correction was used to adjust for multiple comparisons to maintain an overall Type I Error level of 5%.

Isolation of lipids from bacteria

Broth cultures of *E. coli* and *S. aureus* were incubated with each of 0.14 M NaCl (negative control), D-sphingosine, dihydrosphingosine, and phytosphingosine at 500 μg/ml (total volume of treatment was 5 ml per sample) for 4 h at 37°C. Sodium azide (0.05%) was added to kill the bacteria before pelleting by centrifugation. Whole cell pellets were frozen at -80°C, lyophilized, and lipids extracted using a previously described method [22] that consisted of successive extractions with chloroform-methanol mixtures (2:1, 1:1, and 1:2) for two h each at room temperature. Extracted lipids were recovered by evaporation of the solvent under a stream of nitrogen. The lipids were then redissolved in 5 ml chloroform:methanol (2:1), and washed with 1 ml 2 M potassium chloride to remove salts and other water soluble materials [23]. The resulting upper phase was discarded and the lower phase was again dried under nitrogen. Dried lipids were weighed and reconstituted in chloroform-methanol, 2:1 at a concentration of 10 mg/ml. Additional controls included suspensions of each treatment lipid in bacterial growth media (MHB) without bacteria followed by centrifugation and resuspension in chloroform-methanol (2:1) to test the ability of the sphingoid bases to sediment.

Lipid analysis

The lipids from each treatment and control were analyzed for sphingoid bases by quantitative thin-layer chromatography (QTLC) as previously described [24]. Chromatograms were developed with chloroform:methanol:water (40:10:1). Developed chromatograms were sprayed with 50% sulfuric acid and charred by heating slowly to 220°C on a hotplate. Digital images were obtained using a Hewlett-Packard Scanjet 3500c and analyzed using TNIMAGE (Thomas Nelson, Bethesda, MD) in strip densiometry mode to estimate the total extracted lipid weight in each of the treated and untreated bacterial samples as well as controls. Percentage of lipid uptake for each sample was calculated by dividing the total extracted lipid weight by the total weight of lipid added. Sphingosine served as a standard for quantification [25].

Results

Scanning electron microscopy

Control *E. coli* were 2.04 ± 0.46 μm long (mean ± standard error of the mean) by 0.63 ± 0.03 μm wide in size and exhibited typical rod morphology [26]. In contrast, *E. coli* treated with sphingoid bases were distorted and their surfaces were concave and rugate (Fig. 1). Many cells had external blebs. *E. coli* treated with sphingoid bases were notably smaller in length and width when compared with the controls. *E. coli* treated with D-sphingosine were 1.33 ± 0.24 μm long by 0.52 ± 0.03 μm wide; dihydrosphingosine were 1.23 ± 0.29 μm long by 0.59 ± 0.07 μm wide; and phytosphingosine were 1.82 ± 0.73 μm long by 0.73 ± 0.03 μm wide in size (Table 1).

The Kruskal-Wallis test for *E. coli* ($p<0.0001$) was significant at the 5% level of significance, indicating that the distribution of visual surface areas differed among the treatment groups. Post-hoc pairwise comparisons of treatment for *E. coli* and the associated treatments (Table 2) indicated that dihydrosphingosine and sphingosine had distributions of visual surface areas that significantly differed from control ($p=<0.0001$ for both) after multiple comparisons adjustments using an overall 5% level of significance. They did not, however, significantly differ from each other ($p=0.6784$). There was no evidence that the distribution of visual surface areas differed between phytosphingosine and control. Additionally, dihydrosphingosine and sphingosine were each significantly different from phytosphingosine ($p <0.0001$ for both) after multiple comparisons adjustment. Both had medians which are less than that observed with phytosphingosine treatment.

Control *S. aureus* were 0.74 ± 0.03 μm in diameter (± standard error of the mean) and had a typical Gram-positive coccus morphology and staphylococcal arrangement. *S. aureus* treated with sphingoid bases were also distorted to various degrees. Some cells were concave and rugate and appeared to be in various stages of lysis with compromise of the cell wall and plasma membrane. Some cells in clusters were lysed leaving remnants of the cell wall and cellular debris near adjacent cells (Fig. 1). Septal grooves appeared to be more pronounced and deeper than in the control *S. aureus* cells. *S. aureus* treated with D-sphingosine were 0.59 ± 0.08 μm in diameter; cells treated with dihydrosphingosine were 0.57 ± 0.07 μm in diameter; while cells treated with phytosphingosine were 0.73 ± 0.12 μm in diameter (Table 1). The Kruskal-Wallis test for *S. aureus* ($p<0.0001$) was significant at the 5% level of significance, indicating treatment differences in the distribution of visual surface area.

After adjustment for multiple comparisons using the Bonferroni method, post-hoc pairwise comparisons among *S. aureus* and the related treatments (Table 3) also indicated that dihydrosphingosine and sphingosine had smaller visible surface areas that were different from the control ($p<0.0001$ for both). They did not, however, significantly differ from each other ($p=0.2993$). There was no evidence that the distribution of visual surface areas differed between phytosphingosine and control. Additionally, dihydrosphingosine and sphingosine were each significantly different from phytosphingosine ($p <0.0001$ for both). Both had medians which were less than that of phytosphingosine.

Transmission electron microscopy

In thin sections, control *E. coli* had typical Gram-negative rod morphology [27,28] and the outer envelope, interspace, and cytoplasmic membrane were visible (Fig. 2). In *E. coli* treated with sphingoid bases, the outer envelope and cytoplasmic membrane appeared intact and there was no visual evidence that the bacterial cell walls or membranes were damaged.

Interestingly, in *E. coli* treated with sphingoid bases, there were obvious electron dense intracellular inclusion bodies of various sizes and shapes. In many instances, these bodies

filled the intracellular content of the cells. The remaining cytoplasm was not uniform suggesting aggregation or flocculation of intracellular contents.

In thin sections, *S. aureus* had a typical Gram-positive morphology [29,30] and the cell wall and cytoplasmic membrane were clearly visible. The cytoplasm had a characteristic uniform granularity with an occasional fibrinous-like whirl characteristic of the nucleoid (Fig. 2).

In *S. aureus* treated with sphingoid bases, there were cells in various stages of disintegration and lysis. In some cells, there were intact cell walls and cytoplasmic membranes but the cells contained a flocculated cytoplasm. Septal grooves appeared to be more pronounced and deeper than in the control *S. aureus* cells. Other cells had lysed and there were cross sections of cell wall and cellular debris visible near damaged cells.

Like that seen in *E. coli*, *S. aureus* treated with sphingoid bases also contained electron dense intracellular inclusion bodies of various sizes and shapes that filled the intracellular content of the cells. In some cells there were additional vesicles. Whether these were remnants of cytoplasmic membrane still within the cell wall shell are yet to be determined. The remaining cytoplasm was not uniform also suggesting an aggregation or flocculation of intracellular contents.

Thin layer chromatography

Both *E. coli* and *S. aureus* took up large amounts of sphingosine, phytosphingosine, and dihydrosphingosine relative to controls (Fig. 3). A small amount of each of the sphingoid bases did remain on the tube walls or sediment from the medium upon centrifugation and was present in the control sphingosine, phytosphingosine, and dihydrosphingosine lanes but this was a relatively small amount compared to the lipids extracted from treated bacterial samples. Bacterial counts were completed at the beginning and end of the treatment period and confirmed killing of both *E. coli* and *S. aureus* by all three treatments. After the four-hour treatment period, *E. coli* dropped from 3.6×10^8 CFU/ml to 5.2×10^2 upon treatment with sphingosine, 1.0×10^6 with phytosphingosine treatment, and 6.0×10^2 with dihydrosphingosine treatment. *S. aureus* went from 2.2×10^8 CFU/ml in the untreated control to 5.0×10^2 with sphingosine treatment, 3.0×10^4 with phytosphingosine treatment, and 2.0×10^5 upon treatment with dihydrosphingosine.

Discussion

An extensive number of host innate immune factors induce extensive ultrastructural damage to Gram-negative and Gram-positive bacterial cells. These factors include anionic peptides [31], cathelicidins [32], and defensins [29,30]. We report here that sphingoid bases, which have been shown to be antimicrobial by our group and others [13,33,34], also induce extensive ultrastructural damage to *E. coli* and *S. aureus*.

Treated cells from both species were distorted and, in some instances, were notably smaller in size. Their outer surfaces were concave and rugate in appearance, suggesting damage to the cell. Treated cells of *S. aureus* also had a noticeable loss of the cell wall. In thin sections of *E. coli*, there was no evident compromise of bacterial cell walls and membranes appeared to be intact. In *S. aureus*, there was the obvious disruption and loss of cell wall and membrane. Treated cells of both *E. coli* and *S. aureus* contained unique internal inclusion bodies. Hence, lipids at the skin surface induce both extracellular and intracellular damage.

Our results are similar to other studies of sphingoid bases against *S. aureus* in that sphingosine and dihydrosphingosine interfere with cell wall synthesis [13]. Dihydrosphingosine-treated *S. aureus* has multiple lesions in the cell wall, evaginations in

the plasma membrane, and a loss of ribosomes in the cytoplasm [13]. The cell wall lesions may be sequelae of the affected plasma membrane. However, while treatment of *E. coli* with sphingosine results in surface bleb formation, the cell wall appears to be intact. Phytosphingosine appears to cause more overt cell wall damage.

Our results are also similar to those obtained when cells are treated with fatty acids or monoglycerides, which do not disrupt the integrity of the bacterial cell. Often there are no visible effects on bacterial cell walls by either scanning electron microscopy or in thin sections examined by transmission electron microscopy. Rather, the site of action appears to be the plasma membrane, which is often partially dissolved or missing. For example, Group B Streptococcus treated with 10 mM monocaprin for 30 min are killed by disintegration of the cell membrane, leaving the bacterial cell wall intact [35]. The plasma membrane and electron transparent granules are gone. Interestingly, there are no visible effects of monocaprin on the bacterial cell wall directly. No changes can be seen by either scanning electron microscopy or in thin sections examined by transmission electron microscopy. Similarly, *C. albicans* treated with capric acid (C10:0) has a disrupted or disintegrated plasma membrane with a disorganized and shrunken cytoplasm [36]. Again, no visible changes are seen in either the shape or the size of the cell wall. Whether there is a general fluidizing effect resulting in leakage of cellular contents or a more specific interaction with membrane components is not yet known.

The exact mechanism of sphingoid base action on the bacterial cell is currently being elucidated. All microorganisms have polar lipids in their cytoplasmic membranes (Gram-positive and Gram-negative bacteria) and the inner leaflet of the outer membrane (Gram-negative bacteria) [37]. It appears likely that lipids may insert into the outer envelope and cytoplasmic membranes of Gram-negative bacteria and the cytoplasmic membranes of Gram-positive bacteria. Direct changes in the physical properties of the bacterial membranes resulting from sphingoid base insertion may render the membrane non-functional and thus may be the basis for bactericidal activity.

Alternatively, lipids may penetrate and accumulate in the cytoplasm. We have shown here that these sphingoid bases are taken up by both *E. coli* and *S. aureus* in large quantities and there is a possibility that they may be contributing to the internal inclusions seen in our micrographs. Microorganisms are known to accumulate lipid inclusions and microcompartments of varying shapes and compositions. Triacylglycerol inclusions and neutral storage lipid inclusions are just two examples [38,39]. In the case of sphingoid bases, the presence of these lipids may interfere with cell metabolism. It is possible that the sphingoid bases may specifically inhibit certain enzymes in a manner similar to that by which they inhibit mammalian protein kinase C [40].

It is interesting to note that D-sphingosine, dihydrosphingosine, and phytosphingosine induced differing effects on *E. coli* and *S. aureus.* Pairwise comparisons across lipid treatments and controls for each bacterium were significant between the controls and each of dihydrosphingosine and sphingosine but not for phytosphingosine. When comparing lipid treatments, phytosphingosine was different from dihydrosphingosine and sphingosine, but sphingosine and dihydrosphingosine showed no significant differences from each other. Sphingosine and dihydrosphingosine have similar structures, differing by only a single trans double bond. The molecular structure of phytosphingosine, however, contains an additional hydroxyl group, making it more polar. This could also explain the high variability seen in the visual surface area differences of both *E. coli* and *S. aureus* when treated with phytosphingosine. The increased hydrophilicity of phytosphingosine may contribute to slower partitioning into the bacterial membrane.

Increase in *S. aureus* skin colonization is associated with lipid deficiencies. For example, both deficient hexadecanoic acid production [41] and decreased levels of sphingosine [42] are associated with atopic dermatitis and subsequent increase in *S. aureus* skin colonization. Additionally, failure to clear *S. aureus* skin infections within innate immunodeficient mice is linked to mutation of an enzyme necessary for palmitic and oleic acid production [43]. Understanding the specific activities of skin lipids on bacteria contributes to knowledge of the roles of lipids in the control of bacteria on the skin.

In this study, we show that sphingoid bases induce unique ultrastructural damage. Sphingoid base-treated *E. coli* exhibited intact membranes and multiple internal inclusion bodies. Sphingoid base-treated *S. aureus* had obvious membrane and cell wall damage as well as multiple internal inclusion bodies. In conclusion, sphingoid bases commonly found on skin and in mucosal secretions have differential antimicrobial activity against Gram positive and Gram negative bacteria and may have potential for prophylactic or therapeutic intervention of infection.

Acknowledgments

We thank Bonny Olson and Alissa Villhauer for their help with this project. This work was supported by funds from R01 DE018032 and R01 DEO14390 from the National Institute of Dental and Craniofacial Research, National Institutes of Health.

References

1. Brogden NK, Mehalick L, Fischer CL, et al. The Emerging Role of Peptides and Lipids as Antimicrobial Epidermal Barriers and Modulators of Local Inflammation. Skin Pharmacol Physiol. 2012; 25:167–181. [PubMed: 22538862]
2. Jungersted JM, Hellgren LI, Jemec GB, et al. Lipids and skin barrier function--a clinical perspective. Contact Dermatitis. 2008; 58:255–262. [PubMed: 18416754]
3. Bu S, Yamanaka M, Pei H, et al. Dihydrosphingosine 1-phosphate stimulates MMP1 gene expression via activation of ERK1/2-Ets1 pathway in human fibroblasts. FASEB J. 2006; 20:184–186. [PubMed: 16278291]
4. Shi L, Bielawski J, Mu J, et al. Involvement of sphingoid bases in mediating reactive oxygen intermediate production and programmed cell death in Arabidopsis. Cell Res. 2007; 17:1030–1040. [PubMed: 18059378]
5. Saba JD, Hla T. Point-counterpoint of sphingosine 1-phosphate metabolism. Circ Res. 2004; 94:724–734. [PubMed: 15059942]
6. Spiegel S, Milstien S. The outs and the ins of sphingosine-1-phosphate in immunity. Nat Rev Immunol. 2011; 11:403–415. [PubMed: 21546914]
7. Spiegel S, Milstien S. Sphingosine-1-phosphate: an enigmatic signalling lipid. Nat Rev Mol Cell Biol. 2003; 4:397–407. [PubMed: 12728273]
8. Darges JW, Robinson SP, Adams LM. Inhibition of leukotriene B4 (LTB4) in human neutrophils by L-threo-dihydrosphingosine. Adv Exp Med Biol. 1997; 400A:387–392. [PubMed: 9547581]
9. Kim S, Hong I, Hwang JS, et al. Phytosphingosine stimulates the differentiation of human keratinocytes and inhibits TPA-induced inflammatory epidermal hyperplasia in hairless mouse skin. Mol Med. 2006; 12:17–24. [PubMed: 16838068]
10. Pavicic T, Wollenweber U, Farwick M, et al. Anti-microbial and -inflammatory activity and efficacy of phytosphingosine: an in vitro and in vivo study addressing acne vulgaris. Int J Cosmet Sci. 2007; 29:181–190. [PubMed: 18489348]
11. Drake DR, Brogden KA, Dawson DV, et al. Thematic review series: skin lipids. Antimicrobial lipids at the skin surface. J Lipid Res. 2008; 49:4–11. [PubMed: 17906220]
12. Bibel DJ, Aly R, Shinefield HR. Antimicrobial activity of sphingosines. J Invest Dermatol. 1992; 98:269–273. [PubMed: 1545135]

13. Bibel DJ, Aly R, Shah S, et al. Sphingosines: antimicrobial barriers of the skin. Acta Derm Venereol. 1993; 73:407–411. [PubMed: 7906449]
14. Klee SK, Farwick M, Lersch P. The effect of sphingolipids as a new therapeutic option for acne treatment. Basic Clin Derm. 2007; 40:155–166.
15. Bibel DJ, Aly R, Shinefield HR. Antimicrobial activity of sphingosines. J Invest Dermatol. 1992; 98:269–273. [PubMed: 1545135]
16. Bibel DJ, Aly R, Shinefield HR. Inhibition of microbial adherence by sphinganine. Can J Microbiol. 1992; 38:983–985. [PubMed: 1464071]
17. Bibel DJ, Aly R, Shah S, et al. Sphingosines: antimicrobial barriers of the skin. Acta Derm Venereol. 1993; 73:407–411. [PubMed: 7906449]
18. Fischer CL, Drake D, Dawson DV, et al. Antibacterial activity of sphingoid bases and fatty acids against gram-positive bacteria and gram-negative bacteria. Antimicrob Agents Chemother. 2011
19. Klein E, Smith DL, Laxminarayan R. Hospitalizations and deaths caused by methicillin-resistant Staphylococcus aureus, United States, 1999-2005. Emerg Infect Dis. 2007; 13:1840–1846. [PubMed: 18258033]
20. Petkovsek Z, Elersic K, Gubina M, et al. Virulence potential of Escherichia coli isolates from skin and soft tissue infections. J Clin Microbiol. 2009; 47:1811–1817. [PubMed: 19357208]
21. Dryden MS. Complicated skin and soft tissue infection. J Antimicrob Chemother. 2010; 65(Suppl 3):iii35–44. [PubMed: 20876627]
22. Wertz PW, Swartzendruber DC, Madison KC, et al. Composition and morphology of epidermal cyst lipids. J Invest Dermatol. 1987; 89:419–425. [PubMed: 3668284]
23. Folch J, Lees M, Sloane Stanley GH. A simple method for the isolation and purification of total lipides from animal tissues. J Biol Chem. 1957; 226:497–509. [PubMed: 13428781]
24. Wertz PW, Downing DT. Free sphingosines in porcine epidermis. Biochim Biophys Acta. 1989; 1002:213–217. [PubMed: 2930769]
25. Weerheim A, Ponec M. Determination of stratum corneum lipid profile by tape stripping in combination with high-performance thin-layer chromatography. Arch Dermatol Res. 2001; 293:191–199. [PubMed: 11380152]
26. Henk WG, Todd WJ, Enright FM, et al. The morphological effects of two antimicrobial peptides, hecate-1 and melittin, on *Escherichia coli*. Scanning Microsc. 1995; 9:501–507. [PubMed: 8714745]
27. Bayer ME, Carlemalm E, Kellenberger E. Capsule of *Escherichia coli* K29: ultrastructural preservation and immunoelectron microscopy. J Bacteriol. 1985; 162:985–991. [PubMed: 3888968]
28. Bayer ME, Thurow H. Polysaccharide capsule of *Escherichia coli*: microscope study of its size, structure, and sites of synthesis. J Bacteriol. 1977; 130:911–936. [PubMed: 400798]
29. Harder J, Bartels J, Christophers E, et al. Isolation and characterization of human beta -defensin-3, a novel human inducible peptide antibiotic. J Biol Chem. 2001; 276:5707–5713. [PubMed: 11085990]
30. Shimoda M, Ohki K, Shimamoto Y, et al. Morphology of defensin-treated *Staphylococcus aureus*. Infect Immun. 1995; 63:2886–2891. [PubMed: 7622209]
31. Brogden KA, De Lucca AJ, Bland J, et al. Isolation of an ovine pulmonary surfactant-associated anionic peptide bactericidal for *Pasteurella haemolytica*. Proc Natl Acad Sci U S A. 1996; 93:412–416. [PubMed: 8552650]
32. Kalfa VC, Jia HP, Kunkle RA, et al. Congeners of SMAP29 kill ovine pathogens and induce ultrastructural damage in bacterial cells. Antimicrob Agents Chemother. 2001; 45:3256–3261. [PubMed: 11600395]
33. Bibel DJ, Aly R, Shinefield HR. Topical sphingolipids in antisepsis and antifungal therapy. Clin Exp Dermatol. 1995; 20:395–400. [PubMed: 8593716]
34. Payne CD, Ray TL, Downing DT. Cholesterol sulfate protects *Candida albicans* from inhibition by sphingosine in vitro. J Invest Dermatol. 1996; 106:549–552. [PubMed: 8648192]
35. Bergsson G, Arnfinnsson J, Steingrimsson O, et al. Killing of Gram-positive cocci by fatty acids and monoglycerides. APMIS. 2001; 109:670–678. [PubMed: 11890570]

36. Bergsson G, Arnfinnsson J, Steingrimsson O, et al. In vitro killing of *Candida albicans* by fatty acids and monoglycerides. Antimicrob Agents Chemother. 2001; 45:3209–3212. [PubMed: 11600381]

37. Brogden, KA. Cytopathology of pathogenic prokaryotes. In: Cheville, N., editor. Ultrastructural Pathology: The Cellular Basis of Disease. Ames, IA: Blackwell Publishers; 2009. p. 425-524.

38. Alvarez HM, Steinbuchel A. Triacylglycerols in prokaryotic microorganisms. Appl Microbiol Biotechnol. 2002; 60:367–376. [PubMed: 12466875]

39. Kalscheuer R, Stoveken T, Malkus U, et al. Analysis of storage lipid accumulation in *Alcanivorax borkumensis*: Evidence for alternative triacylglycerol biosynthesis routes in bacteria. J Bacteriol. 2007; 189:918–928. [PubMed: 17122340]

40. Hannun YA, Loomis CR, Merrill AH Jr, et al. Sphingosine inhibition of protein kinase C activity and of phorbol dibutyrate binding in vitro and in human platelets. J Biol Chem. 1986; 261:12604–12609. [PubMed: 3462188]

41. Takigawa H, Nakagawa H, Kuzukawa M, et al. Deficient production of hexadecenoic acid in the skin is associated in part with the vulnerability of atopic dermatitis patients to colonization by *Staphylococcus aureus*. Dermatology. 2005; 211:240–248. [PubMed: 16205069]

42. Arikawa J, Ishibashi M, Kawashima M, et al. Decreased levels of sphingosine, a natural antimicrobial agent, may be associated with vulnerability of the stratum corneum from patients with atopic dermatitis to colonization by *Staphylococcus aureus*. J Invest Dermatol. 2002; 119:433–439. [PubMed: 12190867]

43. Georgel P, Crozat K, Lauth X, et al. A toll-like receptor 2-responsive lipid effector pathway protects mammals against skin infections with gram-positive bacteria. Infect Immun. 2005; 73:4512–4521. [PubMed: 16040962]

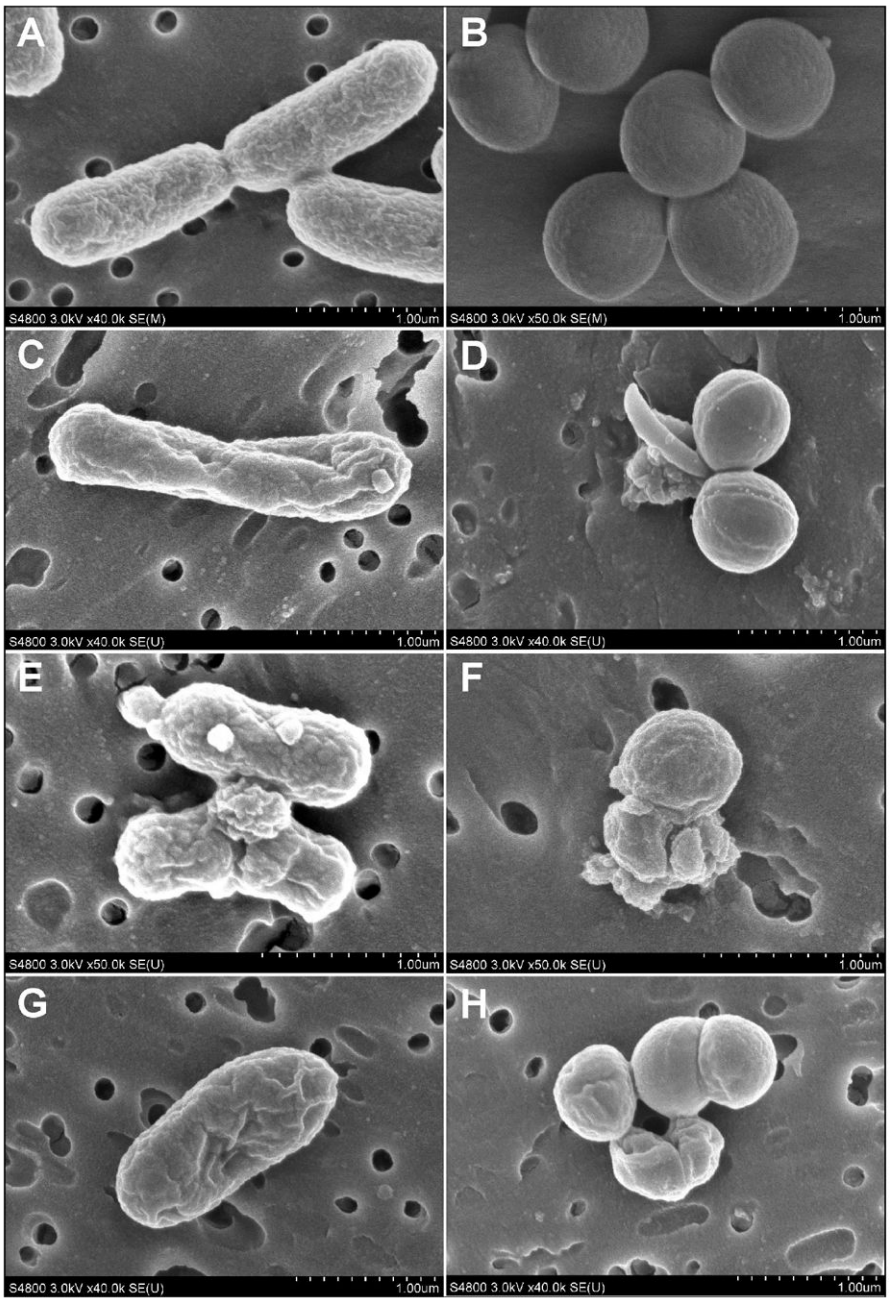

Fig. 1.

SEM images of *E. coli* (left panel) and *S. aureus* (right panel) treated with sphingoid bases (phytosphingosine: C-D; sphingosine: E-F; dihydrosphingosine: G-H). *E. coli* treated with sphingoid bases were distorted and their surfaces were concave and rugate, with many external blebs. *S. aureus* treated with sphingoid bases were also distorted with some cells appearing concave. Many cells were in various stages of lysis with compromise of the cell wall and plasma membrane.

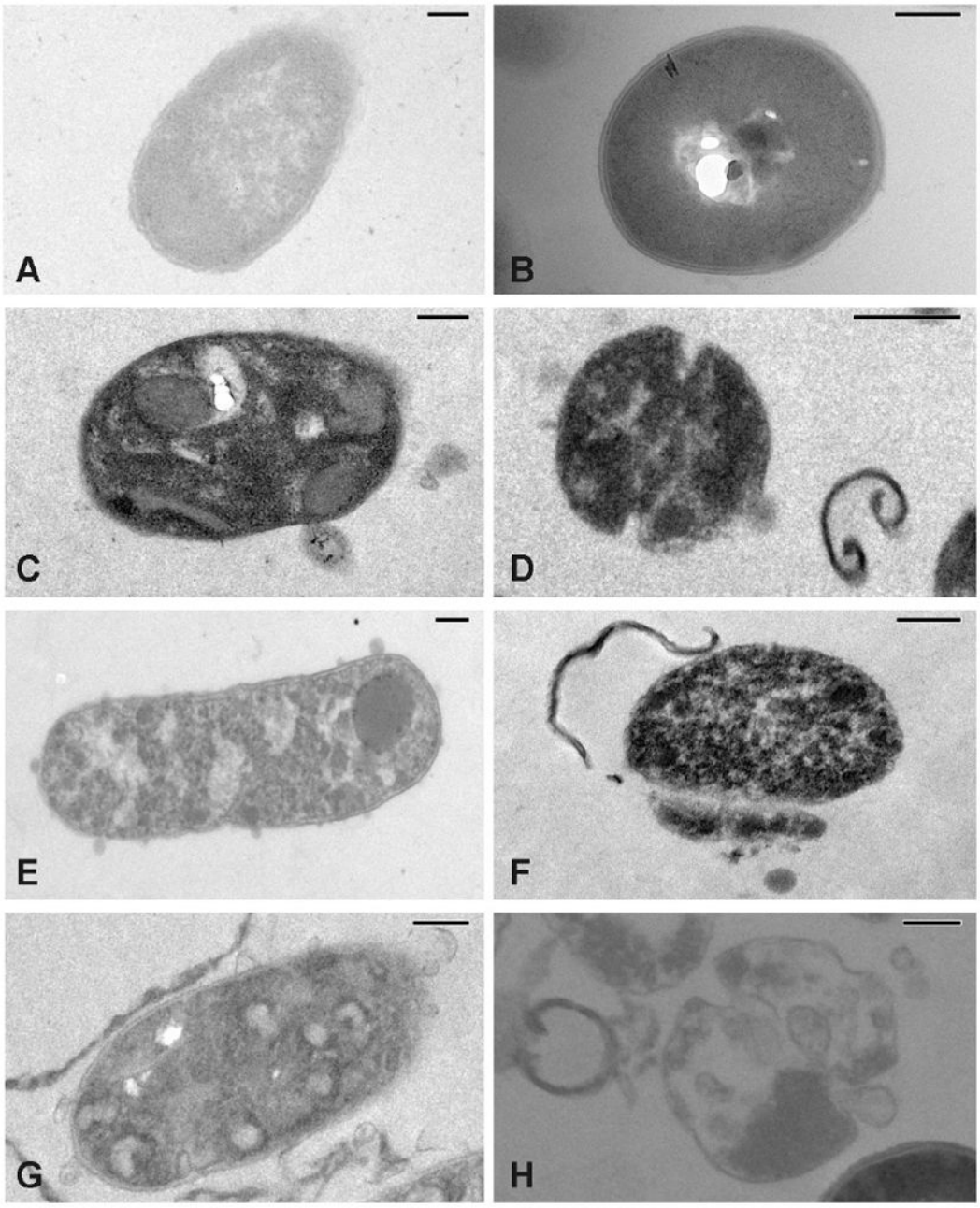

Fig. 2.

TEM images of *E. coli* (left panel) and *S. aureus* (right panel) untreated controls (A-B) and treated with sphingoid bases (phytosphingosine: C-D; sphingosine: E-F; dihydrosphingosine: G-H). Size bars are equal to 0.2 μm. *E. coli* treated with sphingoid bases contained electron dense intracellular bodies not present in the control bacteria and the remaining cytoplasm was not uniform, suggesting flocculation of the intracellular contents. *S. aureus* treated with sphingoid bases also contained electron dense intracellular inclusion bodies with aggregation of the remaining intracellular contents. Cells were also in various stages of disintegration and lysis with sections of cell wall and cellular debris visible near damaged cells.

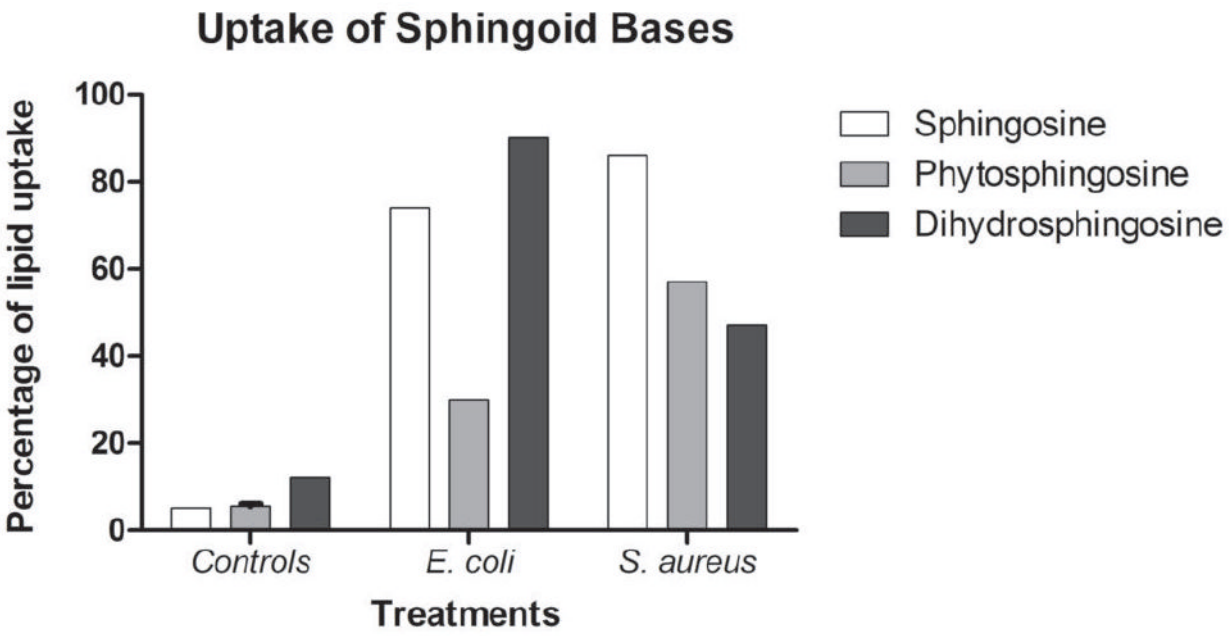

Fig. 3.

Densiometry measurements of the carbon present in the sphingosine standard lanes of TLC chromatograms were used to estimate the total extracted lipid weight in each of the treated and untreated bacterial samples as well as controls. Percentage of lipid uptake for each sample was calculated by dividing the total extracted lipid weight by the total weight of lipid added. Both *E. coli* and *S. aureus* took up a large percentage of the added sphingoid bases relative to controls. Controls included sphingosine (white bar), phytosphingosine (gray bar), and dihydrosphingosine (black bar) in media to ensure that they would not sediment without true bacterial association.

Table 1

Descriptive statistics for the visual surface areas of *E. coli* and *S. aureus* for each of three treatments and controls.

Visual Surface Areas	*E. coli* (μm^2)			*S. aureus* (μm^2)		
	N	Mean (SD)	Median	N	Mean (SD)	Median
Dihydrosphingosine	13	0.663 (0.147)	0.658	25	0.218 (0.017)	0.128
Phytosphingosine	10	1.300 (0.291)	1.356	33	0.128 (0.033)	0.215
Sphingosine	11	0.681 (0.105)	0.684	30	0.215 (0.069)	0.135
Control	11	1.302 (0.318)	1.215	10	0.140 (0.038)	0.219

Table 2

Pairwise exact Wilcoxon Rank Sum comparisons for *E. coli* and treatment comparisons. The Bonferroni correction was used to adjust for multiple pairwise comparisons to maintain an overall significance level of 0.05.

***E. coli* – Pairwise Comparisons**					
Treatment 1	**Median 1**	**Treatment 2**	**Median 2**	**α**[a]	**P-value**
Dihydrosphingosine	0.658	Control	1.215	0.0084	<0.0001[b]
Phytosphingosine	1.356	Control	1.215	0.0084	0.9725
Sphingosine	0.684	Control	1.215	0.0084	<0.0001[b]
Phytosphingosine	1.356	Dihydrosphingosine	0.658	0.0084	<0.0001[b]
Sphingosine	0.684	Dihydrosphingosine	0.658	0.0084	0.6784
Sphingosine	0.684	Phytosphingosine	1.356	0.0084	<0.0001[b]

[a] Bonferroni corrected significance level

[b] Significant after adjustment for pairwise multiple comparisons

Table 3

Pairwise exact Wilcoxon Rank Sum comparisons for *S. aureus* and treatment comparisons. The Bonferroni correction was used to adjust for multiple pairwise comparisons to maintain an overall significance level of 0.5.

***S. aureus* - Pairwise Comparisons**					
Treatment 1	**Median 1**	**Treatment 2**	**Median 2**	**α** [a]	**P-value**
Dihydrosphingosine	0.128	Control	0.219	0.0084	0.0001[b]
Phytosphingosine	0.215	Control	0.219	0.0084	1.0000
Sphingosine	0.135	Control	0.219	0.0084	<0.0001[b]
Phytosphingosine	0.215	Dihydrosphingosine	0.128	0.0084	<0.0001[b]
Sphingosine	0.135	Dihydrosphingosine	0.128	0.0084	0.2993
Sphingosine	0.135	Phytosphingosine	0.215	0.0084	<0.0001[b]

[a] Bonferroni corrected significance level

[b] Significant after adjustment for pairwise multiple comparisons